Decoding of motor imagery involving whole-body coordination

Huixiang Yang, Kenji Ogawa

Department of Psychology, Graduate School of Humanities and Human Sciences, Hokkaido University

Correspondence should be addressed to:

Dr. Kenji Ogawa, Department of Psychology, Graduate School of Humanities and Human Sciences, Hokkaido University, Kita 10, Nishi 7, Kita-ku, Sapporo, 060-0810 Japan

Tel/Fax: +81-011-706-4093

E-mail: ogawa@let.hokudai.ac.jp.

List of abbreviations

MVPA: multivariate pattern analysis

VI: visual motor imagery

KI: kinesthetic motor imagery

MIQ: motor imagery questionnaire

SMC: sensorimotor cortices

M1: primary motor cortex

V1: primary visual cortex

S1: primary somatosensory cortex

SMA: supplementary motor area

PMd: dorsal premotor cortex

PMv: ventral premotor cortex

SPL: superior parietal lobules

IPL: inferior parietal lobules

SVM: support vector machine

Abstract

The present study investigated whether different types of motor imageries can be classified based on the location of the activation peaks or the multivariate pattern analysis (MVPA) of functional magnetic resonance imaging (fMRI) and compared the difference between visual motor imagery (VI) and kinesthetic motor imagery (KI). During fMRI scanning sessions, 25 participants imagined four movements included in the Motor Imagery Questionnaire-Revised (MIQ-R): knee lift, jump, arm movement, and waist bend. These four imagined movements were then classified based on the peak location or the patterns of fMRI signal values. We divided the participants into two groups based on whether they found it easier to generate VI (VI group, n = 10) or KI (KI group, n = 15). Our results show that the imagined movements can be classified using both the location of the activation peak and the spatial activation patterns within the sensorimotor cortex, and MVPA performs better than the activation peak classification. Furthermore, our result reveals that the KI group achieved a higher MVPA decoding accuracy within the left primary somatosensory cortex than the VI group, suggesting that the modality of motor imagery differently affects the classification performance in distinct brain regions.

Keywords

motor imagery, functional magnetic resonance imaging, multi-voxel pattern analysis, Motor Imagery Questionnaire-Revised

Introduction

Motor imagery is defined as the mental simulation or mental rehearsal of movements without any overt motor output (Decety & Jeannerod, 1996; Jeannerod, 2001). Neuroimaging studies in humans demonstrated that motor imagery involves the activation of neural networks engaged in motor execution (Decety et al., 1994; Hanakawa et al., 2003; Parsons et al., 1995) with a similar somatotopic organization of the motor system (Ehrsson et al., 2003; Szameitat et al., 2007a).

Motor imagery involving coordination of the whole body is widely used to facilitate skill acquisition (e.g., Immenroth et al., 2007), enhance motor performance in sports training (e.g., Aymeric Guillot & Collet, 2008), or explore and rehabilitate motor functions (e.g., Braun et al., 2013), and understanding the neural correlates of motor imagery will be useful to optimize sports training or rehabilitation. However, the imagery of general movements is less understood since neuroimaging studies prefer to use simple effector-specific movements that can be executed in a narrow space for the comparison of motor imagery and motor execution, such as motor tasks: hand grasping (Decety et al., 1994), finger tapping (Guillot et al., 2009), manual pointing (Lorey et al., 2010), and foot flexion/extension (Lorey et al., 2014). Furthermore, previous studies reveal that the imagery of hand movements and whole-body (WB) movements recruit different brain regions (Fourkas et al., 2008; Olsson et al., 2008), which suggests that studying motor imagery of effector-specific movement is not sufficient for understanding the functional correlates of motor imagery.

To study general movements, Szameitat (2007b) compared the average of seven upper extremities (UE) movements with the average of seven WB movements, finding that UE activates an inferior part of the sensorimotor cortices (SMC), whereas WB activates a

superior and medial part of the SMC. However, traditional functional magnetic resonance imaging (fMRI) analysis methods lack the resolution to study the imagined movement individually. Recently developed approaches considering patterns of responses across multiple voxels, called multivariate pattern analysis (MVPA), could bypass some of the spatial limitations (Weaverdyck et al., 2020), and Pilgramm et al. (2016) decoded the content of imagined hand movements from the spatial patterns of fMRI data by using MVPA. Therefore, we considered that the MVPA classifier could also be used to study motor imagery of general movements. Moreover, as Friston (2009) pointed out that what could be interpreted from MVPA is the same as univariant analysis, and Ehrsson et al. (2003) proved that the location of activation peaks within the SMCs contains relevant information on the imagined movements, we considered that fMRI signals might also be decoded into imagined movements according to their corresponding peak locations.

Based on the imagery type, previous studies revealed a different neural representation of motor imagery modalities, i.e., between visual-motor imagery (VI) and kinesthetic motor imagery (KI; e.g., Binkofski et al., 2000). Guillot (2009) initially suggested that seeing the movement mentally (visual motor imagery, VI) activates the occipital regions predominantly, whereas feeling the movement mentally (kinesthetic motor imagery, KI) recruits more motor-related regions. However, Hétu (2013) found no significant difference between these two modalities using an activation likelihood estimation (ALE) meta-analysis. Those studies only compared VI and KI using univariant approaches, while MVPA has enhanced sensitivity and finessed characterizations of distributed responses (Friston, 2009). Therefore, we wondered whether the differences between VI and KI could be detected by using MVPA. Considering studies of visual imagery have shown that the primary visual cortex (V1) is critical for visual

imagery (Dijkstra et al., 2017), and studies of tactile imagery have revealed that the primary somatosensory cortex (S1) is associated with mental tactile imagery (Schmidt & Blankenburg, 2019), we focused on the MVPA accuracy within the V1 and S1 to compare the neural correlates of VI and KI.

To sum up, the current study hypothesized that motor imagery of movements involving whole-body coordination could be classified according to brain activity and that some differences may exist between visual motor imagery and kinesthetic motor imagery. We investigated whether and where different imagined movements could be classified from the location of peak activation and spatial patterns, and we further addressed whether the neural differences between VI and KI could be detected by using MVPA.

Materials and methods

Participants

Twenty-five right-handed healthy volunteers (12 men, mean age = 23.64 years old, standard division (SD) = 1.89) participated in the experiment. The study protocol was approved by the local ethics committee of the Center for Experimental Research in Social Sciences at Hokkaido University, and all participants provided written informed consent according to the institutional guidelines before undergoing fMRI scanning.

Movement imagery questionnaire phase

The complete experiment consisted of three phases: (1) movement imagery questionnaire phase, (2) familiarization phase, and (3) fMRI scanning phase.

The present study used the motor items in the MIQ-R (Hall and Martin, 1997), Japanese version (JMIQ-R; Nozomu, 2004). We considered motor items in motor imagery questionnaires as motor imagery tasks since those movements are typical human movements, and we chose MIQ-R rather than newer questionnaires since Nozomi (2004) has validated the Japanese version of the MIQ-R (JMIQ-R) in the Japanese language and population. The JMIQ-R movements are: lifting the right knee, jumping in the air, moving the non-dominant arm, and bending at the waist, each of them requiring the organization of several body parts. There are eight motor imagery items, four from the visual perspective (VI; mentally seeing the movement) and four from the kinesthetic perspective (KI; mentally feeling the movement). For each item in the JMIQ-R, participants first read a description of the start position and the movement (knee lifting, jumping, arm movement, or waist bending). Then, they performed the movement from the start position. After completing the movement, they

were instructed to imagine the movement from VI or KI perspective. Participants were asked to imagine movements with their eyes open to match the motor imagery task during the fMRI experiment. After imagining, they rated the ease of seeing/feeling the movement they had imagined on a 7-point Likert scale ranging from 1 (very difficult to see/feel) to 7 (very easy to see/feel). After completing all motor items in JMIQ-R, participants verbally reported which imagery was more manageable, the VI or KI, without considering any specific individual movement.

Familiarization phase

In the familiarization phase, participants learned to perform the four movements described in the JMIQ-R with simple cues: 1) knee movement, 2) jump, 3) arm movement, and 4) waist movement. All movement cues were restricted to four characters in Japanese to reduce differences between visual stimuli. Participants first learned the correspondence between cues and movements. Then, they completed the four movements with the cues of the four-character Japanese words, which confirmed that they would imagine the correct movements when given the corresponding cues in the fMRI experiment. Participants were then instructed to imagine naturally and relaxedly the four movements in their preferred way, without much consideration for fixing on the VI or KI perspective, as specified in the motor imagery questionnaire. They were asked to imagine all the movements at a fixed frequency—completing one movement every 4 s. At the end of this phase, they completed a training session with the same temporal structure as the fMRI experimental session described below.

fMRI scanning phase

The fMRI scans consisted of four repetitive sessions. Each session contained 20 trials, with five trials for each movement (condition). Conditions were presented in a pseudo-randomized order to avoid presenting the same condition three or more times in a row. At the beginning of each trial, the condition instructions were presented for 4 s, during a period in which the participants were required to imagine that they were ready to initiate the instructed movement. Then, when the orange fixation point appeared, the participants began to imagine performing a set of instructed movements every 4 s for a total of three sets. The number displayed above the fixation was the count of the movement sets. When the fixation turned white, participants were asked to tap the response button once with their right thumb and then relax until the subsequent trial (Figure 1). If no finger response was detected, we considered that the participant failed to complete the task in this trial and discarded the corresponding data.

After the scanning, participants completed a questionnaire about the imagery they created during the fMRI scan. They were asked to rate the degree to which they saw or felt the movement on a 10-point rating scale from 1 (no visual image at all/completely unable to feel) to 10 (there was a complete visual image/feel as if you were performing the movement). The participants also reported their sports experience and motor imagery training experience in the questionnaire.

---------- FIGURE 1 ABOUT HERE ----------

Group division

There is evidence that creating motor imagery is not an easy task for untrained individuals, especially when they are asked to distinguish between VI and KI. For example, Neuper (2005) suggested that mentally feeling movements do not come easily to some individuals,

whereas Hwang (2009) proposed that motor imagery training is needed to help participants create motor imagery. Therefore, instead of asking participants to imagine VI or KI according to their groups, we divide the participants into the VI and KI groups based on their verbal report before the experiment about whether they thought it was easier to perform VI or KI for the analysis (see details in the Results).

MRI acquisition and preprocessing

MRI scans were performed on Siemens MRI Scanner MAGNETOM Prisma (3T) with a 64-channel head coil at Hokkaido University. T2*-weighted gradient echo planar imaging was used to acquire a total of 244 volumes per session (axial slices = 32, slice thickness = 3.5 mm with 4.37 mm gap, repetition time (TR) = 2 s, echo time (TE) = 30 ms, flip angle (FA) = 90°, field of view (FOV) = 192 × 192 mm, matrix = 94 × 94). The orientation of the axial slices was parallel to the anterior commissure–posterior commissure line. The first three volumes within each session were discarded to allow for T1 equilibration. T1-weighted anatomical imaging covering the whole brain was acquired after capturing functional images using a T1 MP-RAGE sequence (axial slices = 224, slice thickness = 0.8 mm without gap, TR = 2300 ms, TE = 2.41 ms, FA = 8°, FOV = 256 × 256 mm^2).

MRI data preprocessing was performed using Statistical Parametric Mapping (SPM12, The Wellcome Centre for Human Neuroimaging). The functional images were first realigned using the least-squares approach and the rigid-body spatial transformation. Then, the realigned functional images and co-registered structural images were spatially normalized to the Montreal Neurological Institute (MNI) space with a final voxel size of $3 \times 3 \times 3$ mm^3

using sinc-interpolation. The scans were smoothed using a Gaussian kernel of 6-mm full width at half-maximum for mass univariate analysis.

Definition of regions of interest

Regions of interest (ROIs) were selected based on previous fMRI studies of motor imagery (e.g., Hétu et al., 2013; Pilgramm et al., 2016). The bilateral primary motor cortex (M1) and S1, supplementary motor area (SMA), and pre-SMA, as well as the dorsal and ventral premotor cortices (PMd and PMv), were defined based on the functional labels obtained from the functional meta-analysis of cortical motor areas (Mayka et al., 2006). Superior and inferior parietal lobules (SPL and IPL) were selected according to the Automated Anatomical Labeling (AAL) atlas (Tzourio-Mazoyer et al., 2002), and V1 was defined as the Brodmann area 17. All voxels within the ROI were used as brain features for training the decoder.

fMRI mass univariate analysis

The fMRI data were analyzed with SPM12 using the General Linear Model. The voxel-wise analysis was performed for boxcar regressors convoluted with a canonical hemodynamic response function. In addition, the six-movement parameters were added to the model as regressors of no interest. Low-frequency noise was removed using a high-pass filter with a 128-s cutoff period. We first analyzed areas significantly activated during the imagery period, regardless of which movement was imagined. The regressors covered the six-volumes (12 s) task period, while both the instruction and button press period were considered part of the baseline. We applied a statistical analysis of the entire brain with a threshold of $p < 0.05$ (family-wise error (FWE) corrected at cluster level with a cluster-

forming threshold of $p < 0.001$ uncorrected). Individual contrast images were generated as imagery > baseline and then modeled as a random effect using the one-sample *t*-test for group analysis.

We then investigated whether the imagery of different movements showed any somatotopic arrangement in the M1, S1, premotor cortex, and SMA. fMRI data were modeled with four regressors corresponding to four movements. Contrast images were calculated as (1) knee, (2) jump, (3) arm, and (4) waist *vs.* all other movements.

Peak coordinate classification and multi-voxel pattern classification

The 20 trials per session were modeled as separate 20 boxcar regressors convolved with a canonical hemodynamic response function using smoothed fMRI data for peak location classification and non-smoothed fMRI data for MVPA classification. Twenty independently estimated parameters per session were calculated for each individual voxel and were then normalized across voxels for each trial. Parameter estimates were subsequently used to identify the imagined movement according to the peak locations and the multi-voxel patterns.

Considering that Ehrsson et al. (2003) showed that motor imagery engages the somatotopic organization in the M1, whereas electroencephalogram studies have classified different motor imagery tasks using features from primary somatosensory areas (e.g., Gouy-Pailler et al., 2008; Pfurtscheller et al., 2006), we hypothesized that imagined movement can be predicted based on the locations of the peak activation within unilateral M1 and S1. We estimated the average prediction accuracy using a four-fold “leave-one-out” cross-validation method, where three sessions were used as training data sets and the other as test data set. The average peak coordinates of each movement in the training set and the peak coordinates

of each trial in the test set were used to classify the imagined movements. We calculated the Euclidean distance between the peak of each experiment in the test set and the peaks of the four movements in the training set, where the movements with the closest distance to the trial peak were used as the predicted category (Euclidean distance method for the peak coordinates classification). We then analyzed the data structure and found that movements are activated with different multi-dimensional Gaussian distributions within the somatosensory regions. We thus added a discriminant analysis method for their classification.

We then performed a linear support vector machine (SVM) on the multi-voxel patterns to discriminate between the four classes of imagined movements. The multi-class classification was conducted using a one-vs-one strategy with the LIBSVM package (Chang & Lin, 2011) with a linear kernel and a cost factor C = 1 to train and test multiple binary classifiers. The four-class dataset was first split into six binary classification datasets and trained separately. The test data was predicted six times, and the model with the most votes was defined as class label. The averaged classification accuracy was estimated with the same fold structure as the peak coordinate classification to obtain the highest sensitivity and specificity.

A one-sample *t*-test across participants in each ROI was performed to determine if the observed classification accuracy was significantly higher than chance (25.0%). Statistical results were corrected for multiple comparisons (number of ROIs) using the Holm-Bonferroni method.

Searchlight analysis

A volume-based searchlight decoding analysis was performed using gray matter voxel patterns within a 9-mm radius sphere. For each iteration, the analysis same as multi-voxel

pattern classification for ROIs was conducted. Classification accuracies were assigned to the central voxel of each sphere. One-sample *t*-tests were performed to subtract clusters where classification accuracy was significantly higher than the chance level (25%) at the group level corrected for the whole brain multiple comparisons with a threshold of $p < 0.05$ and a cluster size of >15. Significant clusters were identified anatomically using the AAL atlas.

Results

Behavioral analysis

The mean score for global JMIQ-R was 6.00 (SD = 0.601), the mean score for VI was 5.87 (SD = 0.96), and the mean score for KI was 6.12 (SD = 0.719). In addition, three participants rated VI higher (i.e., easier) in the JMIQ-R, but KI higher (i.e., easier) after they finished the JMIQ-R, which they claimed was due to their unfamiliarity with the action: the first action in the questionnaire imagined knee movements with KI, and they rated this imagery lower than the other seven imageries. One participant rated KI higher in the questionnaire but verbally reported VI easier later: he/she thought that KI was easier after only finishing the movement. We divided the VI group (n = 10) and KI group (n = 15) according to the participants' reported ease. Because those with inconsistent ratings of ease were asked to confirm whether VI or KI was easier at the reporting stage, we therefore considered self-report to be a better measure of the imagery modality that participants found easier. In addition, we considered that JMIQ-R ratings were related to the prescribed movements, whereas the group division according to self-report provided a more general judgment.

In addition, nine participants reported KI as easier before the fMRI scan but created VI during the experiment. They explained that even though KI was easier to imagine for a given movement, VI saved much more effort than KI when repeating the imagined movement multiple times, so they shifted to imagining seeing the movement (i.e., using VI) during the fMRI experiment. Due to the widely varying sample sizes (19 participants created VI and 6 created KI), we did not analyze the group differences according to the imagery they created during the experiment.

fMRI mass univariate analysis

The activation for all imagined movements in all participants overlapped in the bilateral SMA, M1, and putamen, as well as in the left IPL and right supramarginal gyrus (SMG, Figure 2 and Table 1). Activations revealing the contrast for each movement compared to all other movements are shown in Figure 3 and Table 2. We then compared the VI group with the KI group, and the result showed no significant activation with a cluster-level corrected $p < .05$.

---------- FIGURE 2 & 3 and TABLE 1 & 2 ABOUT HERE ----------

Then, ROI analysis was performed to investigate whether ROIs selected according to previous motor imagery studies were also activated in the present study. One-sample *t*-test was performed to determine whether the estimated parameter changed compared with baseline. The SMA ($t(24) = 3.18$, $p = 0.004$, Cohen's $d = 0.65$) and pre-SMA ($t(24) = 2.17$, $p = 0.04$, Cohen's $d = 0.44$) were significantly activated during motor imagery task. V1 was also significantly negatively activated ($t(24) = -5.81$, $p < 0.001$, Cohen's $d = 1.19$), whereas the averaged activations (parameter estimates) in other ROIs did not differ significantly from the baseline values (Supplementary Figure 1B). The number of activated voxels within each ROIs is shown in Supplementary Figure 1A. Considering our focus on the bilateral activation of M1 and S1, we also plotted their number of activated voxels and estimated parameters separately (Supplementary Figure 2).

Peak coordinate classification

One-way repeated measures analysis of variance (ANOVA) and Tukey's honestly significant difference (HSD) *post-hoc* tests were performed to compare the coordinates of four movements for each dimension. The results showed statistically significant differences for coordinates along the X, Y, and Z axes between movements in the left M1 and S1 (Fs(3, 72) > 3.91, *p*s < 0.012), without significant differences in the right M1 and S1 (Fs(3, 72) < 1.69, *p*s > 0.176). The results of the multiple comparisons showed significant differences between the coordinates of the knee movement and those of the other movements. The averaged peak coordinates for each movement are shown in Figure 4.

---------- FIGURE 4 ABOUT HERE ----------

To test whether the movements could be classified according to their peak coordinates in the bilateral M1 and S1, we compared the classification accuracy against the chance level (25%) using a one-sample *t*-test and the FDR method for multiple comparison correction (Figure 5). The results reveal that the accuracy of classification using a discriminant analysis method exceeded the chance level in the left M1, left S1, and right S1 (*t*s(24) > 2.12, *p*s < 0.048; Table 3), indicating that the imagery contents can be classified through their associated peak coordinates in the SMC.

---------- FIGURE 5 and TABLE 3 ABOUT HERE ----------

As the ANOVA result only suggested differences between the knee movement and the others, we calculated confusion matrices of classification accuracies to determine the percentage of correct classifications for each movement (Figure 6). The matrices showed that

using the discriminant analysis method, the knee movement in the left M1 and the arm movement in the right S1, as the participants imagined their right knee and left arm movement, achieved 35% classification accuracy (Figure 6B). In addition, the diagonal elements of the left S1 were found to be brighter than the other classifications, indicating that the proportion of correct over misleading predictions was greater. The confusion matrices thus provided an intuitive proof that the imagery content can be classified by the peak coordinates of the left M1 and bilateral S1.

---------- FIGURE 6 ABOUT HERE ----------

Multi-voxel classification analysis

We next compared the decoding accuracy in each ROI against the chance level to test whether the imagined movements can be classified using activation patterns. The result showed significantly higher-than-chance classification accuracies in the bilateral M1, S1, pre-SMA, SMA, PMd, PMv, SPL, IPL, and V1 (Supplementary Figure 3).

The decoding accuracy of the bilateral M1 and S1 is shown in Figure 5 for comparison with the peak coordinates analysis. The confusion matrices of the bilateral M1 and S1 calculated from the MVPA classification results are presented in Figure 6C. The comparisons reveal that the classification accuracy using MVPA *vs* peak coordinates is much higher, and this is in line with our expectation that MVPA can provide considerably more information.

A mixed ANOVA with Tukey's HSD *post-hoc* test was conducted to assess the influence of the group as an independent factor and of the ROI as a within-subjects factor on the MVPA decoding accuracy (Figure 7). Group factor included two levels (VI group and KI group), and ROI factor consisted of four levels (bilateral S1 and V1). The main effect for ROI (F(3,

69) = 4.17, p = 0.009) and the interaction effect (F(3, 69) = 4.27, p = 0.008) were statistically significant. The multiple comparison test showed a significant difference between the VI group (mean = 31.25, SD = 5.30) and KI group (mean = 40.75, SD = 12.43) on the left S1 (F(1, 92) = 6.08, p = 0.016), indicating that 15 participants who considered KI easier achieved a significantly higher decoding accuracy within their left S1, whereas no significant difference was found in their other three ROIs (Fs(1, 92) < 0.7, ps > 0.372). The multiple comparison test also revealed a significant difference among four ROIs on the KI group (F(3, 69) = 5.73, p = 0.001), whereas there was no significant difference among ROIs on the VI group (F(3, 69) = 2.70, p = 0.052).

---------- FIGURE 7 ABOUT HERE ----------

Searchlight analysis

The searchlight analysis was lastly performed to identify clusters in which the imagined movements can be classified according to voxel patterns. The results revealed that imagined movements can be decoded from activation patterns in the bilateral precuneus and M1, left IPL, middle temporal lobule, supramarginal lobule, SMA, and right SPL and S1 (Figure 8 and Table 4).

---------- FIGURE 8 and TABLE 4 ABOUT HERE ----------

Discussion

The present study focused on the decoding of motor imagery involving whole-body coordination. We classified imagined movements using fMRI, measuring brain activity peak location and spatial patterns within the SMCs, compared their performance, and investigated the difference between the VI group (those who considered visual motor imagery easier) and the KI group (those considered kinesthetic motor imagery easier) in their classification accuracy. The results show that the four general movements can be classified based on the peak location and spatial patterns within the SMCs, and motor imagery can be differentiated at the individual movement level using signals from regions in the motor imagery network, such as the M1, S1, premotor cortex, SMA, SPL, IPL, and V1. Furthermore, previous studies suggested that a homuncular organization of the SMCs allows representing the imagining of motor processing for different anatomical divisions of the body (Ehrsson et al., 2003; Gouy-Pailler et al., 2008; Szameitat et al., 2007b). Therefore, we hypothesized that the location of brain activity might classify motor imagery involving different body parts. Using simple signal features as the somatotopic features of motor imagery—the activation peak coordinates, our results show that the imagery content might be classified in primary motor and sensory areas using machine learning algorithms. In addition, our results suggest that unilateral limb movements may be more easily classified than WB movements.

Our results reveal that the classification accuracy of the bilateral S1 is significantly higher than the chance level using peak location and spatial patterns as signal features. Many previous studies did not find significant S1 activity during motor imagery (e.g., Hanakawa, Dimyan, & Hallett, 2008; Mizuguchi, Nakata, & Kanosue, 2016; Szameitat, Shen, & Sterr, 2007; Wei & Luo, 2009; see review in Robert M. Hardwick et al., 2018), whereas some

reported that S1 was significantly activated (e.g., Guillot et al., 2008; Van der Meulen, Allali, Rieger, Assal, & Vuilleumier, 2014). Furthermore, Hétu (2013) suggested that activations are constantly found in the postcentral gyrus using ALE meta-analyses. The results of our mass univariate analysis are consistent with those studies finding significant S1 activation, and more importantly, the above-chance classification accuracy of S1 indicates that motor imagery needs the involvement of S1. Therefore, we thought that S1 might play a crucial role in motor imagery. In addition, the MVPA classification accuracy of the left S1 showed a significant group effect, with the VI group compared to the KI group achieving a higher decoding accuracy. We focused on the S1 because tactile imagery activates the somatotopic organization of S1 (Schmidt & Blankenburg, 2019; Yoo et al., 2003), and Guillot et al. (2009) reported that KI, but not VI, activates S1 bilaterally. Group effects on the S1 classification accuracy suggest that the imagery modalities affect the motor imagery classification accuracy with fMRI multi-voxel pattern analysis. This finding provides an approach to improve the classification accuracy by training the participants to imagine the movement kinesthetically, which could be applied to help individuals learn motor imagery, thus facilitating their efficiency of motor skill learning or rehabilitation.

Our results reveal that the motor imagery can be decoded from V1, even when negatively activated. Previous studies have demonstrated that brain activity increases in attended areas and decreases in not attended areas (Maunsell & Cook, 2002), and Amedi (2005) showed that visual imagery suppresses the activation of sensory processing in the auditory cortex that is unrelated to vision. Therefore, the negative response in the V1 might be interpreted as a suppressive effect from motor-related areas. Furthermore, Bressler (2007) showed that even visual stimuli can induce negative BOLD responses within the visual cortex and that these

negative responses still contain valuable information for visual processing. This is consistent with our finding that during motor imagery, the negative responses within V1 are still informative and therefore can be used to classify motor imagery.

Our decoding results agree with Monaco et al. (2020), which suggested that the content of VI and KI can be decoded from the activity patterns of V1. Previous studies directly comparing VI with KI did not show any V1 activation (Guillot et al., 2009; Lee et al., 2019), which was confirmed by the results of our mass univariate analysis. We focused on the visual cortex because visual imagery can be decoded from activity patterns in V1 even if its brain activity does not exceed baseline (Koenig-Robert & Pearson, 2019; Naselaris et al., 2015). However, decoding accuracy was not significantly higher in the VI group than in the KI group, suggesting functions for V1 beyond creating visual images of movement. This might be related to the role of V1 in motor tasks. There is growing evidence that V1 is involved in motor-related functions, such as action planning and execution (Gallivan et al., 2019; Gutteling et al., 2015). Moreover, Mizuguchi et al. (2016) showed that V1 activity is associated with the ability to imagine kinesthetically WB movements. Another possibility is that the V1 plays an essential role in working memory, which is necessary for the completion of motor imagery tasks, and as suggested by Albers et al. (2013), mental imagery and working memory share a joint representation in the early visual cortex.

The searchlight results suggest that the patterns of activity within the M1, S1, SPL, SMA, SMG, precuneus, middle temporal gyrus, and superior occipital gyrus allow distinguishing four types of imagined movements, indicating that information on the different motor imageries can be obtained from the activation patterns in specific regions that form a spatially distributed network. Among these regions, only the SMA, M1, and SMG showed significant

activation during motor imagery, suggesting that the regions activated in different movements do not necessarily show a general increase at the univariate level. Furthermore, the SMA, M1, and IPL were previously found to be consistently activated during motor imagery (Hanakawa, 2016) and are thought to be part of the sensorimotor network. Moreover, the SMG contributes to phonological processing (Gough et al., 2005) and plays an essential role in visual word recognition (Stoeckel et al., 2009). Considering that the condition instructions were Japanese words and the cue words for each movement differed from the others, we considered it reasonable that the SMG was activated during motor imagery and could distinguish between the four movements. Furthermore, ROI analysis but not searchlight analysis showed above chance classification accuracy in V1, indicating that a larger rather than a smaller range of activation patterns in V1 contains more information for classifying various imagined movements.

Moreover, our mass univariate analysis suggests that the different types of motor imagery were indistinguishable on a univariate level, in agreement with the findings by Pilgramm et al. (2016). Furthermore, we failed to predict movement classes using the nearest Euclidean distance, indicating that different movements may elicit similar neural representations on a univariate level. However, using the location of peak activation within SMCs as the feature signal and discriminant analysis as the classification algorithm, imagined movements were distinguishable. Therefore, we consider the location of the activation peaks within the SMC as containing relevant information on the type of imagined movements.

We asked participants to imagine the movements naturally for the following reasons. First, intentionally generated motor imagery is not a commonly used cognitive function for healthy individuals without experience in sports or playing musical instruments. These have been

confirmed by the results of the questionnaire used in the present study. Although all participants conceptualized motor imagery and imagined some movements under the experimenter's guidance, only 7 of the 25 participants had experience with the conscious imagery of movement. In addition, we were unable to assess whether the participants imagined the movements in the desired way, making it difficult for us to help them learn this new skill by providing feedback. Thus, motor imagery was not a task that participants recruited in the current study were able to perform without resistance when let alone intentionally employing visual imagery or kinesthetic imagery. Second, motor imagery was challenging to be supervised by an external observer (i.e., the experimenter), and whether the motor imagery task was performed during the experiment depended entirely on the participant. The experimenter cannot confirm that participants were creating the same motor imagery when given the same movement instructions. Therefore, reducing the resistance to completing a motor imagery task is critically important, especially in repetitive and sometimes monotonous fMRI experiments. Third, reducing the difficulty can reduce the resistance in completing the motor imagery task and thus allow individuals with unlike capacities to perform diverse motor imagery modalities. For these three reasons, we asked participants to imagine the movements naturally to reduce resistance to imagining movements in fMRI experiments, thereby increasing the likelihood that they would complete the motor imagery task well.

Our results illustrated that the neural responses corresponding to different conditions within the ROI differ in two aspects: the spatial distribution of neural signals and the signal values assigned to each specific location. However, the weights of the information carried by all voxels within the ROI are not the same, and the pattern of the weights of the information

carried by each voxel varies under different conditions. Future studies should fully consider the specificity of neural signals to train classification models with better performance, and to find more detailed and specific neural representations of the experimental behavior/ cognition. Moreover, one should interpret these results cautiously since the fMRI signal is an indirect measure of neural activation and is vulnerable to within-subject noise, as there is no guarantee that the imagery created by a participant could be exactly the same when repeatedly imagining a particular movement.

Before and after the fMRI experiment, the questionnaire results showed that it was more challenging to complete KI repeatedly during fMRI scanning, even for some participants who found KI easier when naturally imagining the movement. This finding suggested that performing KI during a repetitive experimental process might be more challenging than a single trial. Even after having learned KI prior to the experiment and after being asked to imagine the movement in a kinesthetic way, participants may have unconsciously replaced KI with VI because they felt KI was more effortful, as nine participants self-reported that KI was easier before the fMRI experiment but still used VI during the experiment in our study. Therefore, we recommend that researchers ask participants after the experiment about the imagery they used during the experiment, especially when imagery modality is one of the studied variables. We expected to compare group division approaches, so we estimated motor imagery ability or preference in several ways. However, limited by the small size of the participants, we could only compare one of the relatively balanced grouping methods. Future studies could compare VI and KI more closely by using more sophisticated grouping methods rather than asking participants to imagine movements visually or kinesthetically.

Conclusion

The present study indicates that motor imagery involving whole-body coordination can be classified based on the location of the related peak activation within the SMC and the multiple voxel activation patterns within the M1, S1, premotor cortex, SMA, SPL, IPL, and V1. In addition, our results suggest that participants who perceived KI as easier than VI had a significantly higher classification accuracy within the left S1 than participants who instead perceived VI as easier than KI.

Acknowledgements

The authors would like to thank Enago (www.enago.jp) for the English language review.

Declarations of interest: none.

Funding

This work was supported by JSPS KAKENHI Grant Number 16K12440 & 17H04683 to KO and Graduate Grant Program of Graduate School of Letters, Hokkaido University, Japan.

Tables

Table 1: Anatomical regions, peak voxel coordinates, and t-values of observed activations during motor imagery.

Anatomic region	voxels	MNI coordinates			t-value
		x	y	z	
L Supplementary motor area	491	-3	-1	59	8.2
R Supplementary motor area		9	2	65	7.07
L Postcentral cortex		-42	-10	50	6.34
R Insula	441	48	8	5	7.7
R Inferior frontal gyrus		60	11	23	6.95
R Rolandic operculum		45	8	14	6.6
L Inferior Frontal gyrus	103	-48	5	8	7.04
L Precentral cortex		-57	5	23	4.81
L Putamen	93	-21	-1	11	5.91
R Supramarginal gyrus	58	42	-34	44	4.32
R Inferior parietal Lobule		33	-40	44	4.32
R Inferior parietal Lobule		39	-43	53	4.13

MNI, Montreal Neurological Institute; L, left hemisphere; R, right hemisphere.

Table 2: Anatomical regions, peak voxel coordinates, and t-values of observed activations.

Anatomic region	voxels	MNI coordinates			t-value
		x	y	z	
Knee > Others					
L Postcentral cortex	143	-18	-40	68	6.18
L Postcentral cortex		-24	-34	77	5.52
L Superior parietal gyrus		-18	-58	71	3.87
Jump > Others					
L Supplementary Motor Area	264	-3	2	65	5.74
L Supplementary Motor Area		-9	-4	74	5.37
L Supplementary Motor Area		-6	-7	65	5.36
Arm > Others					
R Precentral cortex	80	30	-4	53	5.96
- (-)		18	2	50	5.25
R Superior parietal gyrus	48	39	-43	59	4.75
R Inferior parietal gyrus		33	-40	53	4.3
Waist > Others					
no voxels exceeded					

MNI, Montreal Neurological Institute; L, left hemisphere; R, right hemisphere.

Table 3: One-sample *t*-test compare accuracies of classification according to peak ccordinates using Euclidean method and discrinimant analysis method, and classification according to MVPA using SVM to 25% chance level.

One-sample *t*-test (N = 25)							
						95% Confidence Interval	
Methods	ROIs	t	Sig. (2-tailed)	FDR	Mean	Lower	Upper
Peak Coordinates	left M1	1.49	0.151	0.29	27.5	24.026	30.974
Euclidean	right M1	0.32	0.751	0.751	25.45	22.551	28.349
	left S1	2.11	0.045	0.181	28.2	25.072	31.328
	right S1	1.27	0.218	0.29	26.2	24.244	28.156
Peak Coordinates	left M1	2.45	0.022	0.048	29.45	25.696	33.204
Discriminant	right M1	-0.56	0.799	0.799	24.65	21.838	27.462
Analysis	left S1	2.41	0.024	0.048	29.3	25.615	32.985
	right S1	2.12	0.044	0.059	27.4	25.064	29.736
MVPA	left M1	4.84	<.001	<.001	37.65	32.258	43.042
SVM	right M1	5.29	<.001	<.001	36.5	32.014	4.0986
	left S1	5.38	<.001	<.001	36.95	32.369	41.531
	right S1	6.53	<.001	<.001	37.25	33.377	41.123

5

Table 4: Searchlight results showing clusters with above chance decoding of four types of imagery movements.

Anatomic region	voxels	MNI coordinates			t-value
		x	y	z	
L Precuneus	214	-9	-49	68	11.41
L Superior parietal gyrus		-24	-55	62	10.56
L Superior parietal gyrus		-15	-58	59	9.33
L Inferior parietal gyrus	25	-36	-43	44	10.18
L Superior frontal gyrus	21	-24	-7	56	9.59
L Precentral gyrus		-30	-1	50	7.02
R Superior parietal gyrus	203	18	-46	68	9.10
R Postcentral gyrus		30	-46	62	8.96
R Precuneus		12	-52	56	8.75
L Middle temporal gyrus	20	-48	-58	11	8.76
L Middle temporal gyrus		-54	-58	2	7.04
R Precuneus	26	15	-73	44	8.48
R Superior Occipital sulcus		27	-73	44	7.70
L Supplementary motor area	69	0	-1	56	8.45
L Supplementary motor area		0	-1	65	8.38
R Superior frontal gyrus		18	-10	71	7.33
R Postcentral gyrus	21	57	-10	26	8.10
R Supramarginal gyrus		57	-19	26	7.26
R Postcentral gyrus		45	-22	41	7.06
R Postcentral gyrus	31	42	-28	53	7.86
R Precentral gyrus		36	-19	47	7.43
R Postcentral gyrus		45	-19	50	7.09
L Supplementary motor area	19	-12	-7	71	7.56
L Paracentral Lobule		-18	-13	68	7.03
L Superior frontal gyrus		-21	-7	62	6.80

MNI, Montreal Neurological Institute; L, left hemisphere; R, right hemisphere.

References

Albers, A. M., Kok, P., Toni, I., Dijkerman, H. C., & De Lange, F. P. (2013). Shared representations for working memory and mental imagery in early visual cortex. *Current Biology*, *23*(15), 1427–1431. https://doi.org/10.1016/j.cub.2013.05.065

Amedi, A., Malach, R., & Pascual-Leone, A. (2005). Negative BOLD differentiates visual imagery and perception. *Neuron*, *48*(5), 859–872. https://doi.org/10.1016/j.neuron.2005.10.032

Binkofski, F., Amunts, K., Stephan, K. M., Posse, S., Schormann, T., Freund, H. J., Zilles, K., & Seitz, R. J. (2000). Broca's region subserves imagery of motion: A combined cytoarchitectonic and fMRI study. *Human Brain Mapping*, *11*(4), 273–285. https://doi.org/10.1002/1097-0193(200012)11:4<273::AID-HBM40>3.0.CO;2-0

Braun, S., Kleynen, M., Van Heel, T., Kruithof, N., Wade, D., & Beurskens, A. (2013). The effects of mental practice in neurological rehabilitation; a systematic review and meta-analysis. *Frontiers in Human Neuroscience*, *7*(JUL). https://doi.org/10.3389/fnhum.2013.00390

Bressler, D., Spotswood, N., & Whitney, D. (2007). Negative BOLD fMRI response in the visual cortex carries precise stimulus-specific information. *PLoS ONE*, *2*(5). https://doi.org/10.1371/journal.pone.0000410

Chang, C. C., & Lin, C. J. (2011). LIBSVM: A Library for support vector machines. *ACM Transactions on Intelligent Systems and Technology*, *2*(3). https://doi.org/10.1145/1961189.1961199

Decety, J., & Jeannerod, M. (1996). Mentally simulated movements in virtual reality: does Fitt's law hold in motor imagery? *Behavioural Brain Research*, *72*(1–2), 127–134. https://doi.org/10.1016/0166-4328(96)00141-6

Decety, J., Perani, D., Jeannerod, M., Bettinardi, V., Tadary, B., Woods, R., Mazziotta, J., & Fazio, F. (1994). Mapping motor representations with positron emission tomography.pdf. *Nature*, *371*(6498), 600–602.

Dijkstra, N., Bosch, S. E., & van Gerven, M. A. J. (2017). Vividness of visual imagery depends on the neural overlap with perception in visual areas. *Journal of Neuroscience*, *37*(5), 1367–1373. https://doi.org/10.1523/JNEUROSCI.3022-16.2016

Ehrsson, H. H., Geyer, S., & Naito, E. (2003). Imagery of Voluntary Movement of Fingers, Toes, and Tongue Activates Corresponding Body-Part-Specific Motor Representations. *Journal of Neurophysiology*, *90*(5), 3304–3316. https://doi.org/10.1152/jn.01113.2002

Fourkas, A. D., Bonavolont, V., Avenanti, A., & Aglioti, S. M. (2008). Kinesthetic imagery and tool-specific modulation of corticospinal representations in expert tennis players. *Cerebral Cortex*, *18*(10), 2382–2390. https://doi.org/10.1093/cercor/bhn005

Friston, K. J. (2009). Modalities, modes, and models in functional neuroimaging. *Science*, *326*(5951), 399–403. https://doi.org/10.1126/science.1174521

Gallivan, J. P., Chapman, C. S., Gale, D. J., Flanagan, J. R., & Culham, J. C. (2019). Selective Modulation of Early Visual Cortical Activity by Movement Intention. *Cerebral Cortex*, *29*(11), 4662–4678. https://doi.org/10.1093/cercor/bhy345

Gough, P. M., Nobre, A. C., & Devlin, J. T. (2005). Dissociating linguistic processes in the left inferior frontal cortex with transcranial magnetic stimulation. *Journal of Neuroscience*, *25*(35), 8010–8016. https://doi.org/10.1523/JNEUROSCI.2307-05.2005

Gouy-Pailler, C., Congedo, M., Jutten, C., Brunner, C., & Pfurtscheller, G. (2008). Model-based source separation for multi-class motor imagery. *European Signal Processing Conference*, *57*(2), 469–478.

Guillot, A., & Collet, C. (2008). Construction of the Motor Imagery Integrative Model in Sport: a review and theoretical investigation of motor imagery use. *International Review of Sport and Exercise Psychology*, *1*(1), 31–44. https://doi.org/10.1080/17509840701823139

Guillot, A., Collet, C., Nguyen, V. A., Malouin, F., Richards, C., & Doyon, J. (2008). Functional neuroanatomical networks associated with expertise in motor imagery. *NeuroImage*, *41*(4), 1471–1483. https://doi.org/10.1016/j.neuroimage.2008.03.042

Guillot, A., Collet, C., Nguyen, V. A., Malouin, F., Richards, C., & Doyon, J. (2009). Brain activity during visual versus kinesthetic imagery: An fMRI study. *Human Brain Mapping*, *30*(7), 2157–2172. https://doi.org/10.1002/hbm.20658

Gutteling, T. P., Petridou, N., Dumoulin, S. O., Harvey, B. M., Aarnoutse, E. J., Leon Kenemans, J., & Neggers, S. F. W. (2015). Action preparation shapes processing in early visual cortex. *Journal of Neuroscience*, *35*(16), 6472–6480.

https://doi.org/10.1523/JNEUROSCI.1358-14.2015

Hall, C. R., & Martin, K. A. (1997). Measuring movement imagery abilities: A revision of the Movement Imagery Questionnaire. *Journal of Mental Imagery*, *21*(1–2), 143–154.

Hanakawa, T. (2016). Organizing motor imageries. *Neuroscience Research*, *104*, 56–63. https://doi.org/10.1016/j.neures.2015.11.003

Hanakawa, T., Dimyan, M. A., & Hallett, M. (2008). *Motor Planning , Imagery , and Execution in the Distributed Motor Network : A Time- Course Study with Functional MRI*. *December*, 2775–2788. https://doi.org/10.1093/cercor/bhn036

Hanakawa, T., Immisch, I., Toma, K., Dimyan, M. A., Gelderen, P. V. A. N., Hallett, M., Immisch, I., Toma, K., Michael, A., Gelderen, P. Van, & Functional, M. H. (2003). *Functional Properties of Brain Areas Associated With Motor Execution and Imagery*. 989–1002.

Hardwick, R. M., Caspers, S., Eickhoff, S. B., & Swinnen, S. P. (2018). Neural correlates of action: Comparing meta-analyses of imagery, observation, and execution. In *Neuroscience and Biobehavioral Reviews* (Vol. 94, pp. 31–44). Elsevier Ltd. https://doi.org/10.1016/j.neubiorev.2018.08.003

Hétu, S., Grégoire, M., Saimpont, A., Coll, M. P., Eugène, F., Michon, P. E., & Jackson, P. L. (2013). The neural network of motor imagery: An ALE meta-analysis. *Neuroscience and Biobehavioral Reviews*, *37*(5), 930–949. https://doi.org/10.1016/j.neubiorev.2013.03.017

Hwang, H.-J., Kwon, K., & Im, C.-H. (2009). Neurofeedback-based motor imagery training for brain-computer interface (BCI). *Journal of Neuroscience Methods*, *179*, 150–156. https://doi.org/10.1016/j.jneumeth.2009.01.015

Immenroth, M., Bürger, T., Brenner, J., Nagelschmidt, M., Eberspächer, H., & Troidl, H. (2007). Mental training in surgical education: A randomized controlled trial. *Annals of Surgery*, *245*(3), 385–391. https://doi.org/10.1097/01.sla.0000251575.95171.b3

Jeannerod, M. (2001). *Neural Simulation of Action : A Unifying Mechanism for Motor Cognition*. *109*, 103–109. https://doi.org/10.1006/nimg.2001.0832

Koenig-Robert, R., & Pearson, J. (2019). Decoding the contents and strength of imagery before volitional engagement. *Scientific Reports*, *9*(1), 1–14.

https://doi.org/10.1038/s41598-019-39813-y

Lee, W. H., Kim, E., Seo, H. G., Oh, B. M., Nam, H. S., Kim, Y. J., Lee, H. H., Kang, M. G., Kim, S., & Bang, M. S. (2019). Target-oriented motor imagery for grasping action: different characteristics of brain activation between kinesthetic and visual imagery. *Scientific Reports*, *9*(1). https://doi.org/10.1038/s41598-019-49254-2

Lorey, B., Naumann, T., Pilgramm, S., Petermann, C., Bischoff, M., Zentgraf, K., Stark, R., & Vaitl, D. (2014). *Neural Simulation of Actions : Effector- Versus Action-Specific Motor Maps Within the Human Premotor and Posterior Parietal Area ? 1225*(October 2012), 1212–1225. https://doi.org/10.1002/hbm.22246

Lorey, B., Pilgramm, S., Walter, B., Stark, R., Munzert, J., & Zentgraf, K. (2010). Your mind's hand: Motor imagery of pointing movements with different accuracy. *NeuroImage*, *49*(4), 3239–3247. https://doi.org/10.1016/j.neuroimage.2009.11.038

Maunsell, J. H. R., & Cook, E. P. (2002). The role of attention in visual processing. *Philosophical Transactions of the Royal Society B: Biological Sciences*, *357*(1424), 1063–1072. https://doi.org/10.1098/rstb.2002.1107

Mayka, M. A., Corcos, D. M., Leurgans, S. E., & Vaillancourt, D. E. (2006). Three-dimensional locations and boundaries of motor and premotor cortices as defined by functional brain imaging: A meta-analysis. *NeuroImage*, *31*(4), 1453–1474. https://doi.org/10.1016/j.neuroimage.2006.02.004

Mizuguchi, N., Nakata, H., & Kanosue, K. (2016). Motor imagery beyond the motor repertoire: Activity in the primary visual cortex during kinesthetic motor imagery of difficult whole body movements. *Neuroscience*, *315*, 104–113. https://doi.org/10.1016/j.neuroscience.2015.12.013

Monaco, S., Malfatti, G., Culham, J. C., Cattaneo, L., & Turella, L. (2020). Decoding motor imagery and action planning in the early visual cortex: Overlapping but distinct neural mechanisms. *NeuroImage*, *218*(May), 116981. https://doi.org/10.1016/j.neuroimage.2020.116981

Naselaris, T., Olman, C. A., Stansbury, D. E., Ugurbil, K., & Gallant, J. L. (2015). A voxel-wise encoding model for early visual areas decodes mental images of remembered scenes. *NeuroImage*, *105*, 215–228. https://doi.org/10.1016/j.neuroimage.2014.10.018

Neuper, C., Scherer, R., Reiner, M., & Pfurtscheller, G. (2005). *Imagery of motor actions: Differential effects of kinesthetic and visual-motor mode of imagery in single-trial EEG*. https://doi.org/10.1016/j.cogbrainres.2005.08.014

Olsson, C.-J., Jonsson, B., Larsson, A., & Nyberg, L. (2008). Motor Representations and Practice Affect Brain Systems Underlying Imagery: An fMRI Study of Internal Imagery in Novices and Active High Jumpers. *The Open Neuroimaging Journal*, *2*(1), 5–13. https://doi.org/10.2174/1874440000802010005

Parsons, L. M., Fox, P. T., Downs, J. H., Glass, T., Hirsch, T. B., Martin, C. C., Jerabek, P. A., & Lancaster, J. L. (1995). *Use of implicit motor imagery for visual shape discrimination as revealed by PET*. *375*(May), 4–8. https://doi.org/https://doi.org/10.1038/375054a0

Pfurtscheller, G., Brunner, C., Schlögl, A., & Lopes da Silva, F. H. (2006). Mu rhythm (de)synchronization and EEG single-trial classification of different motor imagery tasks. *NeuroImage*, *31*(1), 153–159. https://doi.org/10.1016/j.neuroimage.2005.12.003

Pilgramm, S., Haas, B. De, Helm, F., Zentgraf, K., & Stark, R. (2016). *Motor Imagery of Hand Actions : Decoding the Content of Motor Imagery From Brain Activity in Frontal and Parietal Motor Areas*. *93*(October 2015), 81–93. https://doi.org/10.1002/hbm.23015

Schmidt, T. T., & Blankenburg, F. (2019). The Somatotopy of Mental Tactile Imagery. *Frontiers in Human Neuroscience*, *13*, 10. https://doi.org/10.3389/fnhum.2019.00010

Stoeckel, C., Gough, P. M., Watkins, K. E., & Devlin, J. T. (2009). Supramarginal gyrus involvement in visual word recognition. *Cortex*, *45*(9), 1091–1096. https://doi.org/10.1016/j.cortex.2008.12.004

Szameitat, A. J., Shen, S., & Sterr, A. (2007a). Effector-dependent activity in the left dorsal premotor cortex in motor imagery. *European Journal of Neuroscience*, *26*(11), 3303–3308. https://doi.org/10.1111/j.1460-9568.2007.05920.x

Szameitat, A. J., Shen, S., & Sterr, A. (2007b). Motor imagery of complex everyday movements . An fMRI study. *NeuroImage*, *34*, 702–713. https://doi.org/10.1016/j.neuroimage.2006.09.033

Tzourio-Mazoyer, N., Landeau, B., Papathanassiou, D., Crivello, F., Etard, O., Delcroix, N.,

Mazoyer, B., & Joliot, M. (2002). Automated anatomical labeling of activations in SPM using a macroscopic anatomical parcellation of the MNI MRI single-subject brain. *NeuroImage*, *15*(1), 273–289. https://doi.org/10.1006/nimg.2001.0978

Van der Meulen, M., Allali, G., Rieger, S. W., Assal, F., & Vuilleumier, P. (2014). The influence of individual motor imagery ability on cerebral recruitment during gait imagery. *Human Brain Mapping*, *35*(2), 455–470. https://doi.org/10.1002/hbm.22192

Weaverdyck, M. E., Lieberman, M. D., & Parkinson, C. (2020). Tools of the trade multivoxel pattern analysis in fMRI: A practical introduction for social and affective neuroscientists. *Social Cognitive and Affective Neuroscience*, *15*(4), 487–509. https://doi.org/10.1093/scan/nsaa057

Wei, G., & Luo, J. (2009). *Sport expert's motor imagery: Functional imaging of professional motor skills and simple motor skills*. https://doi.org/10.1016/j.brainres.2009.08.014

Yoo, S. S., Freeman, D. K., McCarthyIII, J. J., & Jolesz, F. A. (2003). Neural substrates of tactile imagery: A functional MRI study. *NeuroReport*, *14*(4), 581–585. https://doi.org/10.1097/00001756-200303240-00011

Nozomu Hasegawa (2004). 'Nihongohan undousinzō situmonsi kaiteihan (JMIQ) no sakusei' [Development of the Japanese Motor Imagery Questionnaire-Revised (JMIQ-R)]. Japanese J. Ment. Imag. 2, 25–34. [in Japanese].

Figures

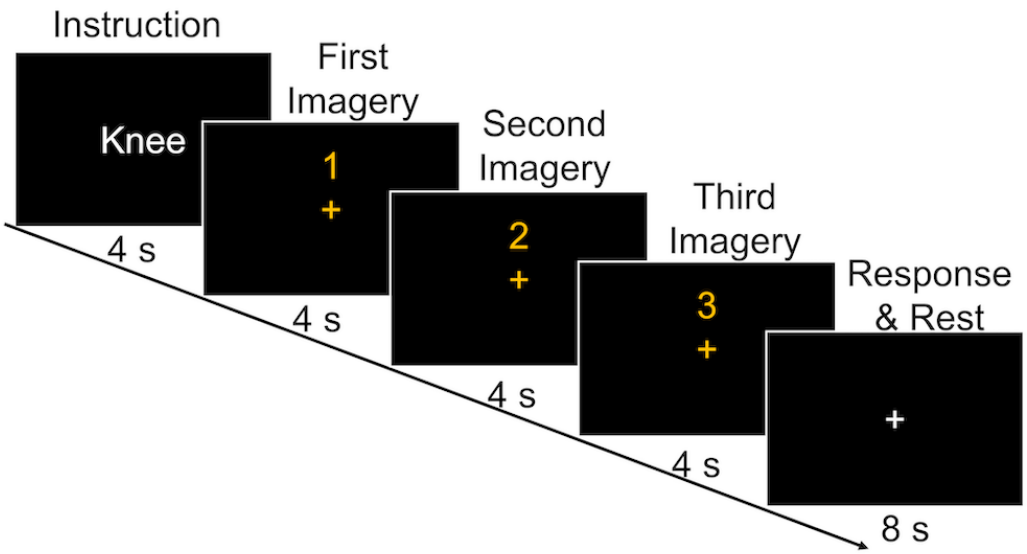

Figure 1:

Schematic depiction of the time course of a single block. First, the visual cue (i.e., four Japanese characters) was displayed, indicating one of the four movements described in the MIQ-R. Four seconds later, an orange fixation was presented, and the participants were asked to start imagining the respective movement three times, every 4 s during the 12-s imagery period. The numbers displayed above the fixation point were counting for the imagery times. When the fixation turned white, the participants were asked to tap the response button once and then to relax until the next block.

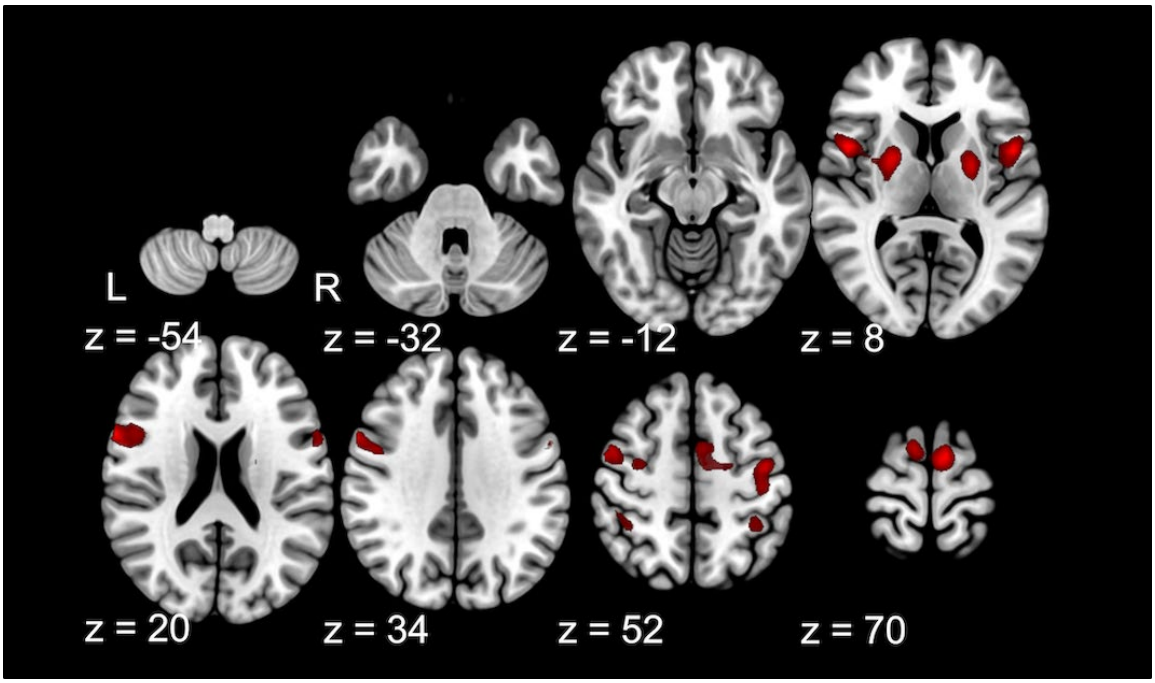

Figure 2:

Regions activated in the mass univariate analysis when imagining all movements. Activation was reported when reaching a threshold of $p < 0.001$ and an extent threshold of $p < .05$ corrected for multiple comparisons. L, left hemisphere; R, right hemisphere. MNI coordinates of activated foci are reported in Table 1. The representation is displayed in the horizontal plane, with Z denoting locations in the MNI coordinates.

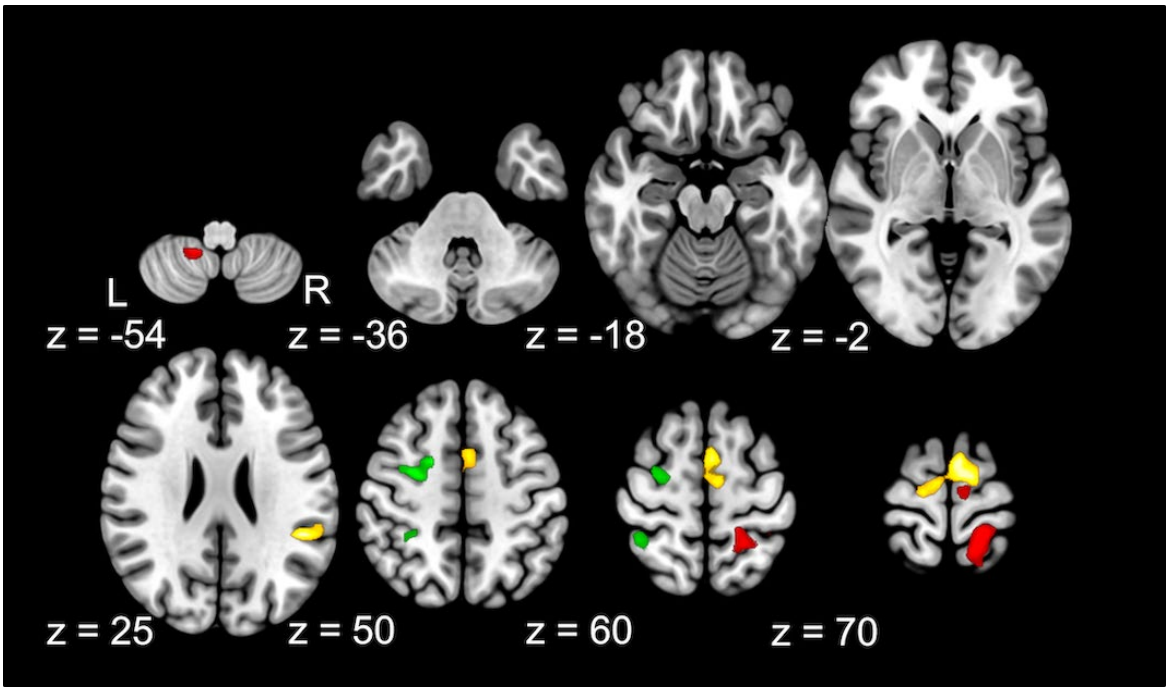

Figure 3:

Regions activated in the fMRI univariate analysis. Red: imagining the knee movement, yellow: jump movement, and green: arm movement *vs* all other movements. Activation was reported when reaching a threshold of $p < 0.001$ and an extent threshold of $p < .05$ corrected for multiple comparisons. L, left hemisphere; R, right hemisphere. MNI coordinates of activated foci are reported in Table 2. The representation is displayed in the horizontal plane, with Z denoting locations in the MNI coordinates.

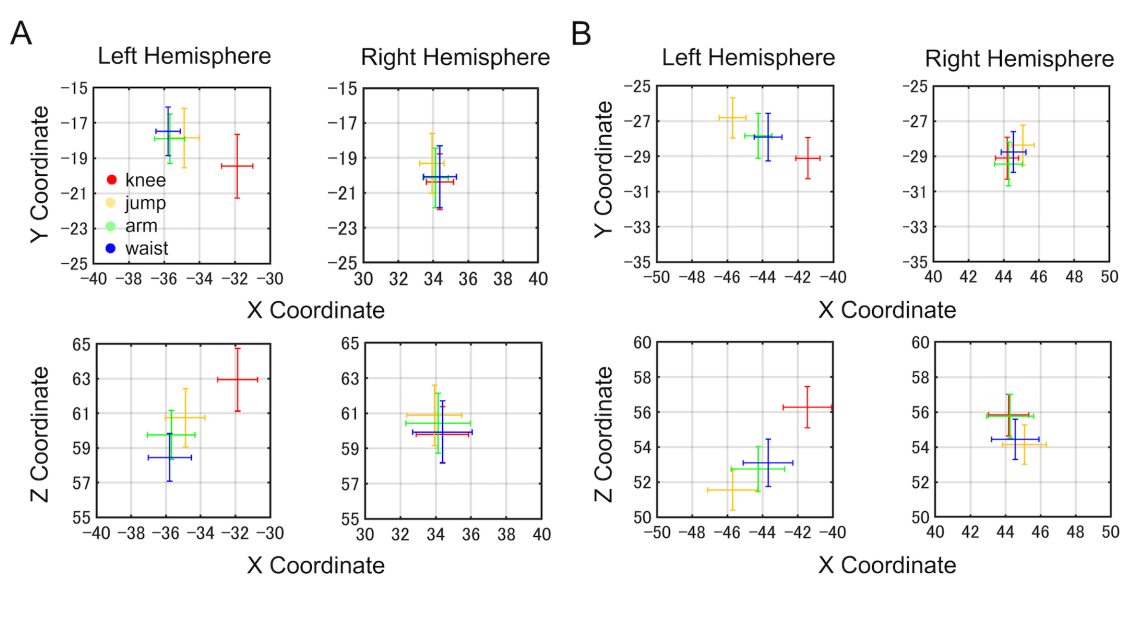

Figure 4:

The peak of activated clusters for each movement, analyzed using mass univariate analysis. (A) Primary motor area and (B) primary somatosensory area. The same sets of coordinates are displayed in x–y planes and x–z planes. Error bars indicate standard errors of the mean.

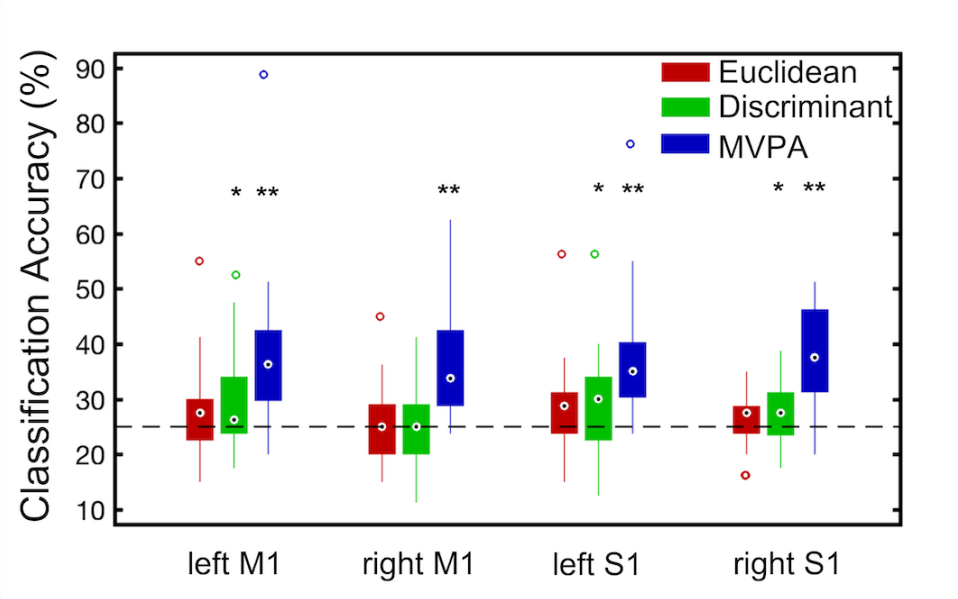

Figure 5:

The averaged peak coordinate classification accuracy and multi-voxel classification accuracy for imagining the four types of movements. M1, primary motor area; S1, primary somatosensory area. The dashed line indicates the chance level (25%). Error bars indicate standard errors of the mean. * $p < 0.05$, ** $p < 0.0001$, FDR <10%.

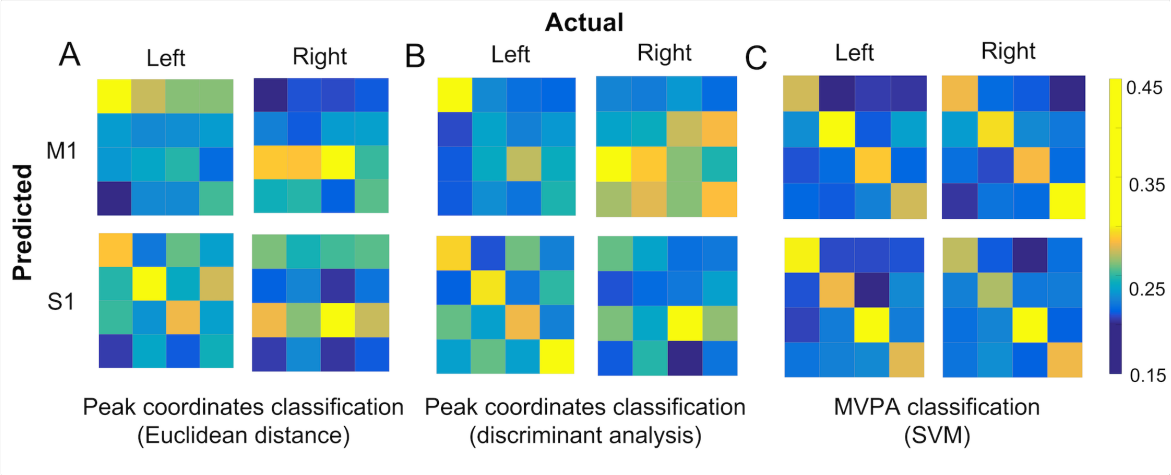

Figure 6:

Confusion matrix of the classification results between each movement, arranged in the order of knee movement, jump, arm movement, and waist movement. (A) Euclidean distance method, (B) discriminant analysis method for peak coordinates classification, and (C) SVM for MVPA. Upper and lower rows represent the results obtained from M1 and S1, respectively; the left and right columns in Figures A, B, and C show the results obtained from the left and right hemispheres, respectively. Each cell represents the percentage ratio (%) of correct classifications determined in each experiment, with the rows and columns representing the predicted and the actual movement, respectively. The diagonal elements represent the classification accuracy (%) for each movement.

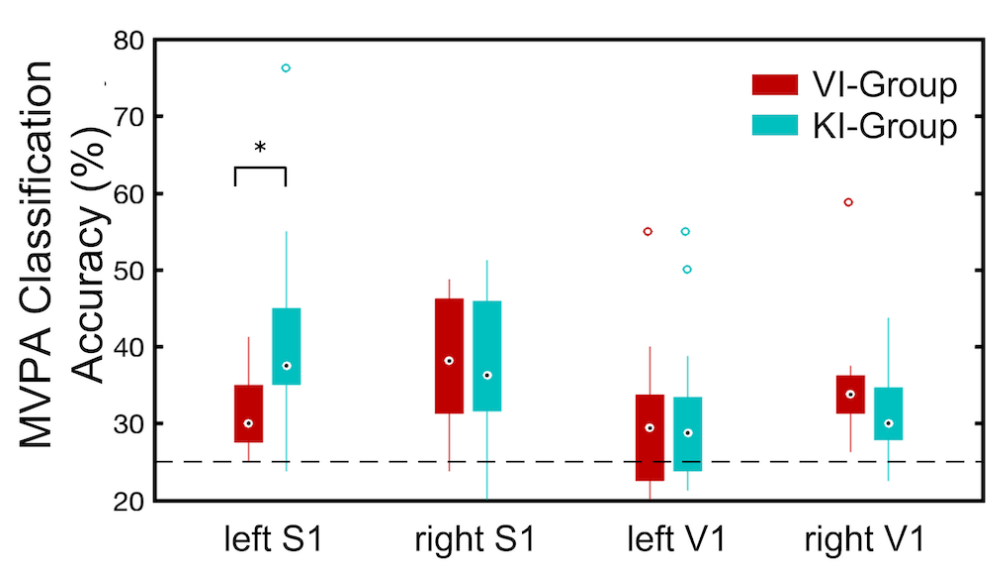

Figure 7:

Averaged MVPA classification accuracies for imagining four types of movements within bilateral S1 and V1 for the VI group and KI group. The dashed line indicates the chance level (25%). Error bars indicate standard errors of the mean. * $p < 0.05$.

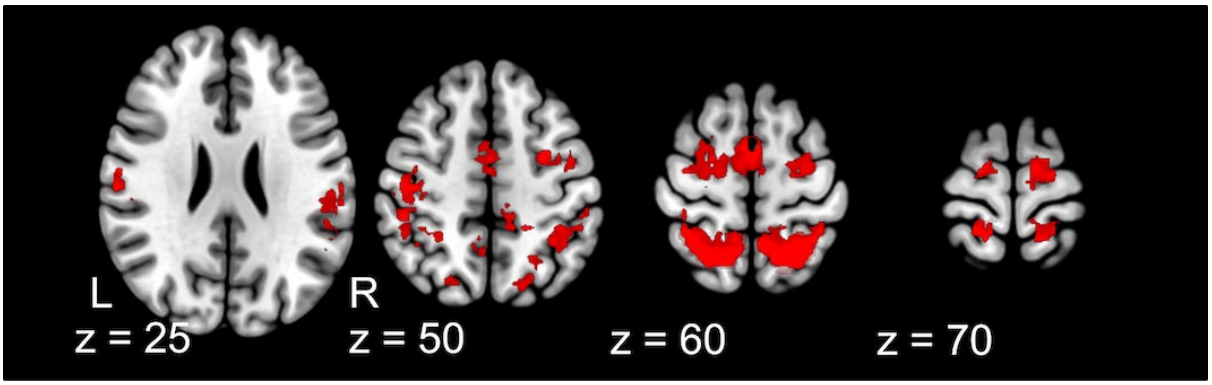

Figure 8:

Decoding performance for four motor imagery classification, with clusters of significant decoding accuracy ($p < 0.05$). FWE corrected at cluster level with an extent threshold of 15 voxels. L, left hemisphere; R, right hemisphere. MNI coordinates of activated foci are reported in Table 4. The representation is displayed in the horizontal plane, with Z denoting locations in the MNI coordinates.

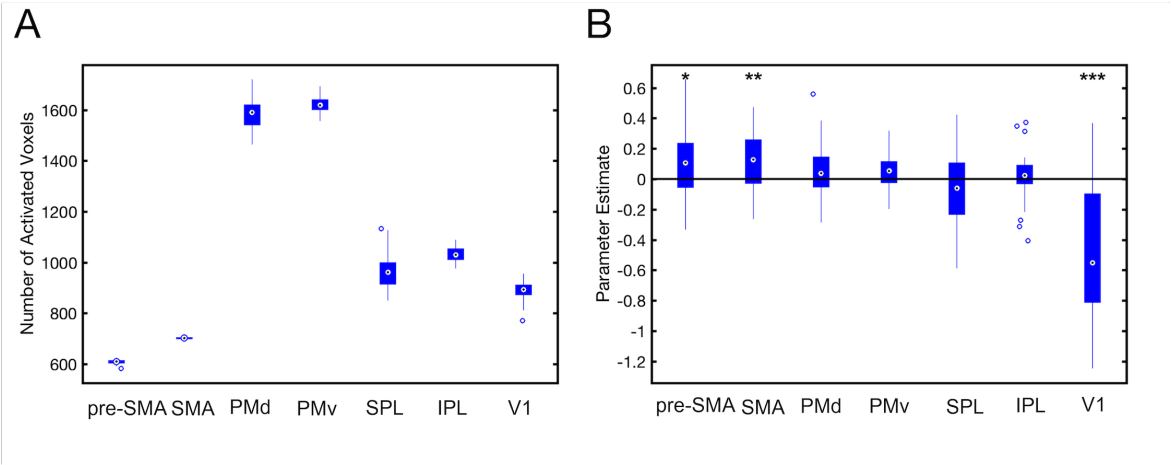

Supplementary Figure 1:

(A) The average number of activated voxels and (B) the averaged activation (parameter estimates) within ROIs. pre-SMA, pre-supplementary motor area; SMA, supplementary motor area; PMd, dorsal premotor cortex; PMv, ventral premotor cortex; SPL, superior parietal lobule; IPL, inferior parietal lobule; V1, primary visual area, defined as Brodmann area 17. Error bars indicate standard errors of the mean.

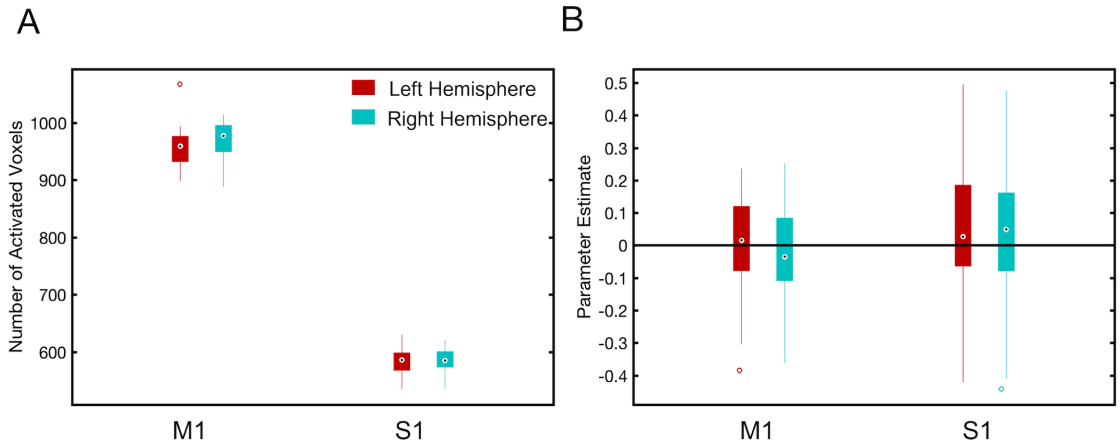

Supplementary Figure 2:

(A) The average number of activated voxels and (B) the average activation (parameter estimates) within ROIs within bilateral M1 and S1. Error bars indicate standard errors of the mean.

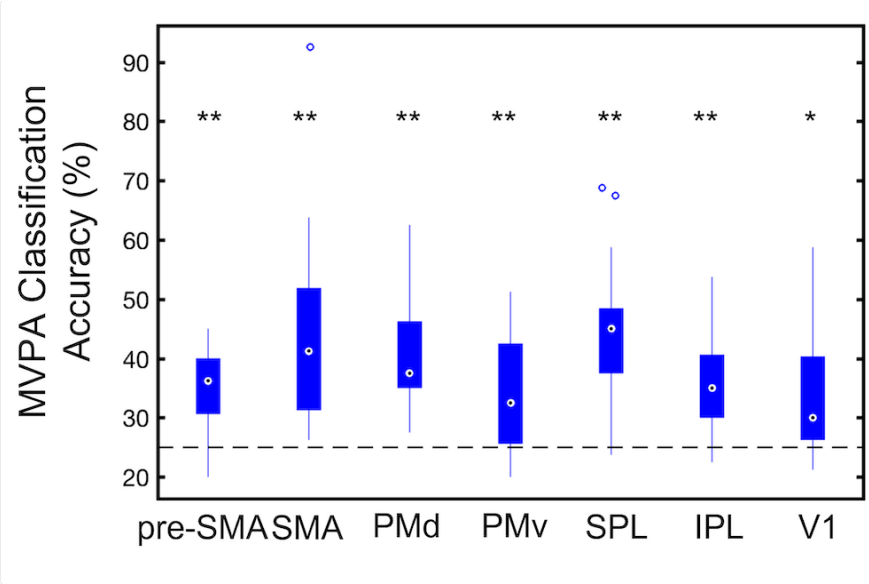

Supplementary Figure 3:

Average classification accuracies for imagining of four types of movements within the ROIs. pre-SMA, pre-supplementary motor area; SMA, supplementary motor area; PMd, dorsal premotor cortex; PMv, ventral premotor cortex; SPL, superior parietal lobule; IPL, inferior parietal lobule; V1, primary visual area, defined as Brodmann area 17. The dashed line indicates the chance level (25%). Error bars indicate standard errors of the mean. * $p < 0.01$, ** $p < 0.0001$.